# ELECTROPHYSIOLOGICAL CHARACTERIZATION OF ATPases IN NATIVE SYNAPTIC VESICLES AND SYNAPTIC PLASMA MEMBRANES

**Petr Obrdlik[*], Kerstin Diekert[*], Natalie Watzke[*], Christine Keipert[*‡], Ulrich Pehl[*], Catrin Brosch[*], Nicole Boehm[*], Inga Bick[*], Maarten Ruitenberg[*§], Walter Volknandt[†] and Bela Kelety[*‖]**

[*] IonGate Biosciences GmbH, Industriepark Hoechst, 65926 Frankfurt/M., Germany
[†] J.W. Goethe Universitaet Biozentrum, AK Neurochemie, 60438 Frankfurt/M., Germany
[‡] present address: Max Planck Institut für Biophysik, 60438 Frankfurt/M., Germany
[§] present address: Merz Pharmaceuticals GmbH, 60318 Frankfurt/M., Germany
[‖] present address: Bela Kelety Consulting, 65931 Frankfurt/M., Germany

Address correspondence to: Petr Obrdlik, Industriepark Hoechst D528, 65926 Frankfurt am Main, Germany, E-mail: petr.obrdlik@iongate.de

## Abstract

Vesicular V-type $H^+$-ATPase (V-ATPase) and the plasma membrane-bound $Na^+/K^+$-ATPase are essential for the cycling of neurotransmitters at synapse, but direct functional studies on their action in native surroundings are limited due to the poor accessibility via standard electrophysiological equipment. We performed solid supported membrane (SSM)-based electrophysiological analyses of synaptic vesicles and plasma membranes prepared from rat brains by sucrose gradient fractionation. Acidification experiments revealed V-ATPase activity in fractions containing the vesicles but not in the plasma membrane fractions. For the SSM-based electrical measurements, the ATPases were activated by ATP concentration jumps. In vesicles, ATP-induced currents were inhibited by the V-ATPase-specific inhibitor bafilomycin A1 (BafA1) and by 4,4'-diisothiocyanatostilbene-2,2'-disulfonic acid (DIDS). In plasma membranes, the currents were inhibited by the $Na^+/K^+$-ATPase inhibitor digitoxigenin. Distribution of the V-ATPase- and $Na^+/K^+$-ATPase-specific currents correlated with the distribution of vesicles and plasma membranes in the sucrose gradient. V-ATPase-specific currents depended on ATP with $K_{0.5}$ of 51 ± 7 µM and were inhibited by ADP in a negatively cooperative manner with $IC_{50}$ of 1.2 ± 0.6 µM. Activation of V-ATPase had stimulating effects on the chloride conductance in the vesicles. Low micromolar concentrations of DIDS fully inhibited the V-ATPase activity, whereas the chloride conductance was only partially affected. In contrast, 5-nitro-2-(3-phenylpropylamino)-benzoic acid (NPPB) inhibited the chloride conductance but not the V-ATPase. The presented data describe electrical characteristics of synaptic V-ATPase and $Na^+/K^+$-ATPase in their native surroundings, and demonstrate the feasibility of the method for electrophysiological studies of transport proteins in native intracellular compartments and plasma membranes.

**Short title:**
Electrophysiology of synaptic V-ATPase and $Na^+/K^+$-ATPase

**Keywords:**
V-ATPase; synaptic vesicles; electrophysiology; solid supported membrane; $Na^+/K^+$-ATPase; chloride conductance;

**Abbreviations:**
V-ATPase, V-type ATPase; SSM, solid supported membrane; BafA1, bafilomycin A1; Dig, digitoxigenin; DIDS, 4,4'-diisothiocyanatostilbene 2,2'-disulfonic acid; NPPB, 5-nitro-2-(3-phenylpropylamino)benzoic acid; CCCP, carbonyl cyanide-m-chlorophenylhydrazone; SV, synaptic vesicles; SPM, synaptic plasma membranes; NMG, N-methylglucosamine.

## Introduction

Electrophysiological studies of transport proteins in their native environment can help to understand the interplay of different ions and solutes at membranes, and its impact on the physiology of the corresponding organs or tissues. At synaptic plasma membranes, $Na^+/K^+$-ATPase builds electrochemical $Na^+$ and $K^+$ gradients, which are the major driving forces for the transport of neurotransmitters from the synaptic cleft into the cytosol [1]. Loading of neurotransmitters into synaptic vesicles is driven by an electrochemical proton gradient built up by a multi-subunit V-type ATPase (V-ATPase) [2, 3]. Beside the V-ATPase, chloride conducting proteins also play an important role in building the optimal proton gradient [4, 5]. Both, the transport of protons via V-ATPases as well as the translocation of $Na^+/K^+$ cations across membranes via $Na^+/K^+$-ATPases generate electrical currents and thus are suited for electrophysiological analysis [6, 7]. However, electric measurements of ATPases in native membranes and intracellular compartments are challenging. Particularly, synaptic vesicles are difficult to access with standard electrophysiological equipment due to their small size (~40 nm). Therefore, the existing electrophysiological studies deal mainly with vesicular channels but synaptic V-ATPase and vesicular transport proteins have not yet been electrically characterized in their native surroundings [8, 9]. On the other hand, direct measurements on plasma membrane $Na^+/K^+$-ATPases are usually performed in excised-out giant patch clamp configuration complicating the electrophysiological analysis [10]. For these reasons, knowledge of electrical properties of synaptic V-ATPase and $Na^+/K^+$-ATPases in their native surrounding is limited.

During the last ten years, the solid supported membrane (SSM) technique was shown to be suited for electrical analysis of transporters, pumps and channels in different membrane environments [7, 11, 12]. For such electrical measurements, the SSM is built on a planar gold electrode by depositing an alkane-thiol layer followed by a phospholipid layer on top of it. Membrane fragments or vesicles containing the protein of interest are then adsorbed onto this SSM (Fig. 1). Thereby, a fluid compartment is formed between the SSM and the protein-containing membranes. The protein-specific charge movements into or out of this compartment are induced by rapid exchange of a non-activating solution for a solution containing either a substrate or a protein-activating agent [11]. Depending on the sign of the moved charges and the direction of the transport either positive or negative transient currents are detected [13]. The transient nature of the currents is based on the arrangement of the adsorbed membranes and SSM on the sensor, and the current detection principle [11]. Briefly, the SSM behaves like a capacitor with the solution in the fluid compartment and the gold electrode beeing the capacitor plates (Fig. 1). According to these arrangements, the transport-dependent transient currents correspond to the charging of the sensor gold electrode and the charging kinetics depends on the transport activity of the assayed protein [7, 11, 13]. In general, the peak current value is used to analyze the protein transport activity.

We applied the SSM-based technique for electrical analysis of ATPases in native synaptic vesicles and synaptic plasma membranes. The specificity of the underlying protein activities was determined by measuring substrate dependencies and by testing V-ATPase and $Na^+/K^+$-ATPase inhibitors. Beside that, the regulation of V-ATPase by ADP was studied. To distinguish between V-ATPase and chloride-specific effects in synaptic vesicles both, the ATP- and chloride-induced currents were characterized with the respective inhibitors.

## Materials and Methods

*Preparation and storage of synaptic vesicles and plasma membranes.* Synaptic vesicles (SV) and synaptic plasma membranes (SPM) were isolated from rat brains via percoll and sucrose gradient centrifugation as described in Morciano et al. [14, 15] with following modifications. One whole brain of an adult Sprague Dawley rat (Harlan, Borchen, Germany) was used per each preparation. The brain was homogenized with a glass homogenizer as described previously, the homogenate was centrifuged for 10 min at 1000 x *g* and 4°C, and the resulting supernatant was layered on a discontinuous percoll gradient (3%, 10%, 23% percoll (v/v) in 5 mM Tris/HCl, 320 mM sucrose, pH 7.4). After 7 min centrifugation at 31000 x *g* the fractions containing synaptosomes (between 3 and 10% and 10 and 23%) were collected and lysed according to the original protocol. The resulting suspension was layered onto a continuous sucrose gradient ranging from 0.3 M to 1.2 M sucrose in 0.5 mM EGTA, 10 mM HEPES/NaOH pH 7.4 of a total volume of 32 ml. The gradient was centrifuged for 2 h at 85000 x *g* and 30 fractions (1 ml each) were collected. Typically, SV were enriched in lower density fractions 5 to 9 and contained around 80 ng/µl total protein. SPM were enriched in fractions 22 to 28 and contained around 200 ng/µl total protein. SV or SPM of

each fraction were divided into 100 µl aliquots equivalent of 8-20 µg total protein, frozen in liquid nitrogen, and stored at -75°C.

*Preparation of biosensors and SSM-based electrical measurements.* The biosensors were prepared with gold-electrode sensors from IonGate Biosciences (Germany) as described by the manufacturer. Briefly, the solid supported membrane (SSM) was built on a gold electrode by applying first an alkane-thiol followed by a phospholipid di-phytanoyl-phosphatidyl-choline. Subsequently, the SSM-coated sensors were covered with 50 µl of equilibration buffer (150 mM KCl, 50 mM Hepes, pH 7.2/NMG, 2 mM $MgCl_2$, 0.2 mM DTT) and incubated at 4°C for 15 min. An aliquot of SV or SPM (5-20 µg of total protein) was thawed and sonicated with a microsonicator by applying 5 bursts with an amplitude of 30% (ultrasonic processor UP 50 H with a MS 1 tip, Dr. Hielscher, Germany). 0.5-2 µg total protein of the sonicated SV or SPM were loaded on each sensor and incubated at 4°C for 12 h. After this incubation the sensors could be stored for another 48 h at 4°C without significant reduction of the protein activities. For electrical measurements, the SV- or SPM-loaded biosensors were integrated into the fluidic system of the *SURFE$^2$R One* setup (Surface Electrogenic Event Reader, IonGate Biosciences, Germany) and the proteins were activated via rapid exchange between pre-incubating, non-activating and activating solutions [11, 13]. The application of activating solution induced transient rapidly decaying currents. After the current decayed, the system was set back by rinsing the sensor with the pre-incubating or non-activating solutions. The proteins were then activated again by applying the non-activating and the activating solution. Like this, different solutions and experimental conditions could be assayed on the same sensor. If required, possible changes (run down) of the protein activity during the experimental period was monitored by application of a reference activating solution. V-ATPase-mediated currents were induced by exchanging the non-activating solution (150 mM K-Asp, 50 mM Hepes, pH 7.2/NMG, 2 mM $MgSO_4$, 10 mM KCl) by the activating solution (non-activating solution supplied with 5 – 300 µM ATP, "ATP-concentration jump"). 0.2 mM DTT was added to stabilize the V-ATPase protein activity. $Na^+/K^+$-ATPase was activated by 5 – 1000 µM ATP in $Na^+$ -containing buffers (140 mM NaCl, 30 mM HEPES, pH 7.0/NaOH, 2 mM $MgCl_2$). Chloride conductance was measured by rapid exchange of a pre-incubating solution (330 mM K-Asp, 50 mM Hepes, pH 7.2/NMG, 2 mM $MgSO_4$) for a non-activating solution (preincubation solution with 300 µM K-ATP) followed by an activating solution (300 mM K-Asp, 50 mM Hepes, pH 7.2/NMG, 2 mM $MgSO_4$, 30 mM KCl, 300 µM K-ATP). Inhibitors were prepared as DMSO stock solutions (DIDS, Baf A1, NPPB) or ethanol stock solutions (digitoxigenin) and added in equimolar amounts to all solutions. The final concentration of DMSO or ethanol in solutions never exceeded 0.1%.

*Acidification assays*. Acidification of membrane vesicles was measured by following the quenching of acridine orange (AO) fluorescence in the fluorescence spectrophotometer (FlexStation, Molecular Devices, USA) with excitation and emission wavelengths at 485 and 530 nm. The reaction buffer contained 60 mM KCl, 10 mM MOPS, pH 7.4/KOH, 4 mM $MgSO_4$, and 300 mM sucrose. Shortly before the experiment, AO (1 mM AO in 30% EtOH) was added to the final concentration of 10 µM, and SV or SPM suspensions were applied at the final total protein concentration of ~0.05 µg/µl. The reaction was started by adding 120 µM K-ATP, and stopped by adding either V-ATPase inhibitors or ionophores. Fluorescence changes were monitored at 37°C.

## Results

*Preparation of synaptic vesicles and membranes, and acidification assays.* The synaptic vesicles (SV) and plasma membranes (SPM) were prepared from whole rat brains using adapted sucrose gradient protocols of Morciano et al. [14, 15]. Using this protocol SV are enriched in lower density fractions 5 to 9, whereas SPM are contained in higher density fractions 22 to 28. We tested the distribution of SV in the low- and high-density fractions by measuring the V-ATPase-mediated acidification of vesicles with the fluorescence dye acridine orange (AO) [16]. In these assays the acidification is detected as the quenching of the AO fluorescence. For the experiments the SV fractions F5 to F9, and the SPM fractions F24 to F26 were each pooled, and the AO fluorescence changes were recorded with the spectrophotometer (FlexStation, Molecular Devices, USA). Adding 120 µM ATP to the reaction mix decreased the AO fluorescence in the SV fractions, but not in the SPM fractions (Fig. 2A). The moderate increase of the fluorescence in SPM fractions was not ATP specific since it was observed also after adding other chemicals such as DMSO (data not shown). In SV the ATP-induced fluorescence decrease was inhibited by the V-ATPase inhibitor bafilomycin A1 (BafA1) at a concentration of 25 nM [17]. In SPM BafA1 had no effect on the AO fluorescence. The pre-incubation of SV with the proton ionophore carbonyl cyanide-m-

chlorophenylhydrazone (CCCP) or with DIDS inhibited the ATP-induced effects (Fig. 2B). Moreover, supplying CCCP after the ATP application reversed the fluorescence quenching, demonstrating that the quenching was due to the accumulation of protons in SV.

*Electrical measurements of the V-ATPase activity.* To measure the electric activity of synaptic V-ATPase, SSM sensors were prepared with the SV-containing fractions (F5 to F9) and the protein was activated by rapid exchange of a non-activating, ATP-free solution for an activating solution containing ATP (ATP concentration jumps). To suppress possible $Na^+/K^+$-ATPase activity due to residual SPM contaminations in SV fractions, the measurements were performed in $Na^+$-free conditions. Consistent with a translocation of positive charges (protons) across the adsorbed SV membranes towards the electrode, the ATP concentration jumps induced positive currents on the SV-loaded sensors (Fig. 3A, [12, 13]). In SSM-based electrophysiology, the protein-dependent currents correspond to the charging of a capacitor formed by the SSM, the fluid compartment and the gold electrode (Fig. 1, [11, 13]). As expected for capacitor charging, the ATP-induced currents were transient and decaying in range of several hundred milliseconds after the application of the activating solution. The time range of the current decay correlated with the SSM-measurements of other transporter proteins [11-13]. As soon as the current decayed completely, the system was set back by equilibrating the sensor in the non-activating solution. The protein could be repeatedly activated by applying the activating solution over an extended time period (4-6 hours) and different experimental conditions could be tested on the same sensor. The ATP concentration jumps induced electrical currents on the synaptic vesicles only in presence of 2 mM $Mg^{2+}$, whereas no ATP-induced currents were observed with solutions lacking $Mg^{2+}$ and containing 0.5 mM EDTA (Fig. 3A). The currents were fully inhibited by BafA1 (25 nM, Fig. 3B), and depended on the ATP concentration with the apparent half maximal concentration $K_{0.5}^{ATP}$ at 51 ± 7 µM (Fig. 3C, D).

*Electrical measurements of the $Na^+/K^+$-ATPase*. For the measurements of the plasma membrane-associated $Na^+/K^+$-ATPase, the sensors were prepared with the higher density fractions (F24 to F28) enriched in SPM. The experiments were performed as described by Pintschovius *et al.* [7] with non-activating and activating solutions containing $Na^+$ but free of $K^+$. On SPM-coated sensors, 150 µM ATP concentration jumps induced fast-decaying electric currents (Fig. 4A). The currents were reduced by the $Na^+/K^+$-ATPase inhibitor digitoxigenin (Dig, 1 µM), whereas 10 nM BafA1 had no effect on the ATP-induced currents of SPM fractions (Fig. 4A, [18]). At 1 µM concentration, Dig inhibited the ATP currents to approximately 20-30%. The remaining currents could be further inhibited by increasing Dig concentrations (data not shown). The Dig-sensitive currents depended on ATP with the calculated $K_{0.5}^{ATP}$ of 12 ± 5 µM (Fig. 4B).

*Distribution of V-ATPase and $Na^+/K^+$-ATPase in sucrose gradient.* The described protocol for the separation of SV and SPM by continuous sucrose gradients was originally applied for proteomic studies and the distribution of V-ATPase, $Na^+/K^+$-ATPase, and other SV and SPM marker proteins was characterized immunologically via western blot [14, 15]. To perform functional analysis of the V-ATPase and $Na^+/K^+$-ATPase distribution in the gradient, the representative SV fractions F6-8, the SPM fractions F24-26 and the intermediate fraction F14 were tested for the V-ATPase and $Na^+/K^+$-ATPase activity by ATP concentration jumps in $Na^+$-free or in $Na^+$-containing solutions, respectively, and by applying the respective inhibitors BafA1 and Dig. Fig. 4C and Suppl. Tab. 1 show the BafA1-sensitive and the Dig-sensitive ATP-induced currents in the different fractions. In SV fractions F6-8 under $Na^+$-free conditions, the ATP-induced currents were inhibited by 10 nM BafA1 but insensitive to Dig. In $Na^+$-containing solutions, the currents were to a minor extent (~18%) also sensitive to 1 µM Dig (Fig. 4C and Suppl. Tab. 1) suggesting some $Na^+/K^+$-ATPase activity in the SV-enriched fractions possibly originating from residual SPM contaminations. In SPM fractions F24-26 the ATP-induced currents were insensitive to BafA1 but inhibited by Dig. No ATP-induced currents were detected with the intermediate fraction F14. Overall, these results correlate with the distribution of the V-ATPase and $Na^+/K^+$-ATPase proteins in the sucrose gradient, as described by immunoblot analysis [14, 15]. Partial Dig sensitivity of the ATP-dependent currents in F6-8 suggested that there may be some residual contamination with $Na^+/K^+$-ATPase (SPM) in SV fractions. To avoid any effects of the $Na^+/K^+$-ATPase, all further V-ATPase studies were performed under $Na^+$-free conditions.

*V-ATPase and kinetics of inhibition with BafA1, DIDS and ADP.* BafA1 inhibits V-ATPases in low nanomolar range, whereas other membrane-bound ATPases are not affected or sensitive only to significantly higher concentrations in the micromolar range [17]. Accordingly, the V-ATPase- but not the $Na^+/K^+$-ATPase-specific currents were inhibited with 10 nM BafA1 supplied to the non-activating and activating solutions (Fig. 4A, C). In previous studies BafA1 was described to accumulate in membranes [19]. Therefore, the effects of different BafA1 concentrations were

studied over an extended period of time. BafA1 at concentrations of 5 and 1 nM also inhibited the V-ATPase-specific currents but longer incubation times were needed (Fig. 5A). The incubation time necessary for the inhibition was dose-dependent with the slowest kinetics at the lowest BafA1 concentration. The BafA1 effects were either not or only poorly reversible under the given experimental conditions. Beside BafA1, 4,4'-diisothiocyanatostilbene 2,2'-disulfonic acid (DIDS), a general inhibitor of chloride conducting proteins, has also been described to inhibit V-ATPases at low micromolar concentrations [16]. To further characterize the V-ATPase-specific currents, DIDS and as a competitive inhibitor ADP were used [16, 20, 21]. For testing DIDS, the inhibitor was added to the non-activating and activating solutions and the V-ATPase activity was recorded for 15 to 50 min (Fig. 5B). Addition of 10 and 1 µM DIDS resulted in a complete inhibition of the V-ATPase-specific currents. Similar to BafA1, the incubation time necessary for the complete inhibition was dose-dependent with slower kinetics at the lower DIDS concentration. After 50 min incubation with 0.1 µM DIDS the V-ATPase activity was reduced by 30% with a further falling tendency suggesting that the inhibition did not reach the maximum. For ADP inhibition experiments, V-ATPase was activated by 120 µM ATP in presence of increasing ADP concentrations in the non-activating and activating solutions. At these conditions, the $IC_{50}$ for ADP was at 1.2 ± 0.6 µM with the Hill coefficient at 0.5 ± 0.1 (Fig. 5C). The reversibility of the ADP effects depended on the applied ADP concentration (Fig. 5D). Whereas low ADP effects (≤1 µM) could not be reversed at the given conditions, the effects of 10 or 100 µM ADP were partially reversible. V-ATPase activities after the washout of 10 or 100 µM ADP both recovered to the V-ATPase activity measured in presence of ~1 µM ADP.

*V-ATPase and vesicular chloride conductance*. Beside the inhibitory effects on V-ATPase, DIDS is a general inhibitor of chloride-conducting proteins [16, 22]. To test if DIDS may also act on the V-ATPase activity through the inhibition of chloride-conducting proteins in SV, protocols were adapted for measuring chloride fluxes on SSM-based biosensors. On SV-loaded sensors, 30 mM $Cl^-$ concentration jumps induced negative electric currents (Fig. 6A). The negative sign of these currents is in agreement with the movement of negative charges (chloride anions) toward the sensor electrode, as opposed by the positive currents induced by the movement of positive charges via the V-ATPase and $Na^+/K^+$-ATPase [13]. Chloride transport into the synaptic vesicles is linked to the V-ATPase activity [4, 5, 23]. Accordingly, the activation of the V-ATPase with 0.3 mM ATP in non-activating and activating solutions resulted in an increase of chloride-induced currents by ~49% (Suppl. Fig. 1, Fig. 6A). The positive currents induced by the ATP concentration jump from pre-incubating to non-activating solution mark the activation of the V-ATPase. DIDS and NPPB are blockers of anion channels and transporters [22]. To test the influence of these inhibitors on chloride-induced currents, either DIDS or NPPB were supplied to the solutions and the measurements were performed as described above. Like in the previous experiments (Fig. 5B) the V-ATPase signal was inhibited by DIDS at low micromolar concentrations (Fig. 6B). The chloride-induced peak currents were reduced by 32 and 45% at 1 and 10 µM DIDS and the level of reduction remained the same between 10 µM and 100 µM DIDS (Fig. 6B, D). In contrast to DIDS, 10 µM NPPB inhibited the chloride currents by 80% but did not affect the V-ATPase-specific currents (Fig. 6C, D).

## Discussion

Electrophysiological measurements are a standard tool for studying the function and the physiology of transporters, pumps and channels at plasma membranes. However, electrophysiological data on intracellular proteins such as V-ATPases, as well as data on electrical properties of plasma membrane-bound $Na^+/K^+$-ATPases in their native surroundings are limited. In this study we used SSM-based biosensors to electrically analyze V-ATPase and $Na^+/K^+$-ATPase in purified synaptic vesicles (SV) and synaptic plasma membranes (SPM).

*Quality of the purified SV and SPM.* In the applied membrane purification protocol, SV accumulate in the low-density sucrose gradient fractions, whereas SPM are concentrated in the higher-density fractions at the bottom of the gradient [14, 15]. The quality of the purified SV was first tested via measuring V-ATPase-dependent acidification using acridine orange (AO) as a pH-sensitive fluorescent dye [16]. On SV-containing low density fractions, ATP induced a decrease of the AO fluorescence that was inhibited by DIDS, by the proton ionophore CCCP and by the V-ATPase inhibitor BafA1. This demonstrates that the measured fluorescence changes were due to the V-ATPase-dependent proton accumulation in the vesicles, thus showing that the low-density fractions are suited for functional studies of V-ATPase activity [2, 3, 16, 17]. No significant AO fluorescence decrease could be detected testing the high density fractions, showing that these

fractions were largely free of vesicle contaminations. The separation of SV and SPM was further tested by analyzing the distribution of the V-ATPase- and $Na^+/K^+$-ATPase-specific electrical activities in the sucrose gradient fractions. Here, the distribution of V-ATPase and $Na^+/K^+$-ATPase activities correlated with the distribution of V-ATPase and $Na^+/K^+$-ATPase proteins in previously published immunoblot assays [14, 15]. In SV-enriched fractions, the minor effects of the $Na^+/K^+$-ATPase inhibitor Dig on the ATP-induced signals suggested some $Na^+/K^+$-ATPase activity due to residual contamination with SPM. However, the use of $Na^+$-free solutions fully suppressed the Dig effects (i.e. $Na^+/K^+$-ATPase activity) and selected specifically for the V-ATPase activity (see also below). Hence, the use of $Na^+$-free conditions should be generally applicable for selective studies of the $Na^+$-independent vesicular transport proteins in SV fractions. All together, the results demonstrate that the applied preparation and the SSM measurement protocols are well suited for functional studies of synaptic vesicles as well as plasma membranes.

*Specificity of the V-ATPase-related currents.* Low-density sucrose gradient fractions containing the purified SV were used for the electrical analysis of synaptic V-ATPase. Several features show that the ATP-induced currents correspond to the V-ATPase activity. First, like other membrane-bound ATPases, V-ATPase needs $Mg^{2+}$ as a cofactor for an efficient ATP hydrolysis [24]. Accordingly, the ATP-induced currents were $Mg^{2+}$-dependent. Second, the currents were sensitive to the inhibitor BafA1 at low nanomolar concentrations, which are highly specific for V-ATPases [17]. In contrast, P-type ATPases are either not affected or are inhibited by BafA1 only at >1000 times higher micromolar concentrations [17]. Third, the absence of $Na^+$ in the experiments demonstrates that the ATP signals cannot originate from the P-type $Na^+/K^+$-ATPase via possible plasma membrane contamination. Fourth, the calculated $K_{0.5}^{ATP}$ of 51 µM is in range of $K_{0.5}^{ATP}$ for other V-ATPases [21, 24, 25]. Together with the fact that the applied SV showed a well-detectable V-ATPase activity in acidification assays, these features demonstrate that the detected electrical currents are V-ATPase-specific.

*Characterization of the $Na^+/K^+$-ATPase-specific currents.* In presence of $K^+$, the $Na^+/K^+$-ATPase pumps three $Na^+$ into the cytosol and two $K^+$ out, thus being electrogenic [1, 10]. In addition, $Na^+/K^+$-ATPase can also conduct electrical currents in $K^+$-free solutions as demonstrated in black lipid membrane (BLM) and SSM experiments [7, 26]. The SSM-based measurements of the synaptic $Na^+/K^+$-ATPase were performed with SPM-enriched sucrose gradient fractions in absence of $K^+$. According to the previously published SSM-based experiments with the pig kidney $Na^+/K^+$-ATPase [7], fast decaying, transient currents were obtained on SPM-loaded sensors upon rapid ATP concentration jumps under $K^+$-free conditions. The ATP-induced currents were inhibited with the membrane-permeable $Na^+/K^+$-ATPase-specific inhibitor digitoxigenin (Dig) demonstrating that the detected currents correspond to the $Na^+/K^+$-ATPase activity [18]. Moreover, the calculated $K_{0.5}^{ATP}$ of ~12 µM was in good agreement with the $K_{0.5}^{ATP}$ of ~3 µM determined for a pig $Na^+/K^+$-ATPase in $K^+$ free solutions [7]. Since ATP can bind to the $Na^+/K^+$-ATPase only from the intracellular side of the protein, these results demonstrate that the applied SPM adsorbed - at least partially - in the inside-out configuration to the sensors. For the $Na^+/K^+$-ATPase, a low affinity and a high affinity ATP binding had been described [27]. ATP binds with low affinity to the $K^+$-bound protein, whereas the high-affinity ATP binding was observed in absence of $K^+$ [28, 29]. Interestingly, the $K_{0.5}^{ATP}$ values determined at $K^+$-free conditions with the SSM-based technique were significantly lower than the $K_m^{ATP}$ of 70 – 460 µM determined for different rat $Na^+/K^+$-ATPase αβ oligomers in presence of $Na^+$ and $K^+$ (this work, [1, 7]). This suggests that the $K_{0.5}^{ATP}$ determined in this work reflects at least partially the high-affinity binding of ATP to the $Na^+/K^+$-ATPase.

*Inhibition of the V-ATPase-specific currents with BafA1 and DIDS.* BafA1 is a highly hydrophobic macrolide antibiotic binding to the membrane spanning domain of the V-ATPase protein [17]. Several independent groups have reported on the reversibility of BafA1 effects on the V-ATPase activity *in vivo* [30, 31]. In such *in vivo* studies, the *de novo* synthesis of the enzyme was postulated to be responsible for the recovery of the activity [19]. *In vitro* studies using reconstituted V-ATPase in liposomes have shown that BafA1 does not bind covalently and that the binding is reversible [32, 33]. However, in these assays the BafA1 binding was reversible only in presence of lipid excess provided by addition of protein-free liposomes. Because of its highly lipophilic nature BafA1 was suggested to accumulate and/or tightly bind to the membranes [17, 19]. This high hydrophobicity might explain why the inhibitory effect of BafA1 on the V-ATPase-specific currents could not be reversed under the here described experimental conditions. Similarly, the time dependence of the BafA1 effect may reflect the accumulation of the inhibitor on the sensors.

The stilbene derivate DIDS had been described to inhibit the synaptic V-ATPase at low micromolar concentrations [16]. The inhibition of proteins by DIDS is often irreversible as DIDS can form covalent bonds with amino groups of amino acids [34, 35]. In our experiments DIDS inhibited the V-ATPase-specific currents at low micromolar concentrations and the inhibition was dose- and time-dependent, and irreversible. The time dependency and the poor reversibility of the DIDS effect on ATP-induced currents suggest that the stilbene derivate may interact with the V-ATPase via covalent bonding.

*Inhibition of the V-ATPase-specific currents with ADP.* Compared to batch-based methods such as acidification assays, the SSM-based approach allows real-time V-ATPase measurements without accumulation of the ATP-hydrolysis products in the experimental solutions. Therefore, the approach is well suited for studying the regulation of the V-ATPase by ADP. The sensitivity of the V-ATPase-specific currents to ADP is in agreement with the general mode of action of V-ATPases, and with ADP being important for the feedback control of V-ATPases [20, 21, 24, 36]. The Hill coefficient of ~0.5 suggests a negative cooperativity of the ADP binding to the V-ATPase protein. This is consistent with the existence of a high-affinity ($K_d$ ~66 nM) and a low-affinity ($K_d$ ~17 µM) ADP binding site in the V-ATPases [37]. In addition to the Hill coefficient, the characteristics of the ADP washout in the SSM-based experiments also suggest that multiple ADP binding sites exist. In these experiments, the inhibition with up to 1 µM ADP was only poorly reversible, which correlates with the dynamic range of the high-affinity ADP binding [37]. In contrast, the recovered V-ATPase-specific currents obtained after the washout of higher ADP concentrations (10 or 100 µM) approximated to values corresponding to the currents measured in presence of 1 µM ADP. This suggests that the high-affinity binding of ADP to the enzyme was poorly reversible under the respective experimental conditions, whereas ADP at the low-affinity binding site(s) could be well washed out.

*V-ATPase activity and chloride conductance.* Chloride serves as the counter anion of protons and plays an important role in acidification of SV and endosomes [4, 22]. In agreement with the $H^+$ and $Cl^-$ ions being electrochemically coupled, the chloride-induced currents of SV were significantly increased in presence of an activated V-ATPase. DIDS is a general inhibitor of chloride conducting proteins, but it also inhibits synaptic V-ATPase at low micromolar concentrations [16]. The inhibition profile of ATP- and chloride-induced currents suggested that DIDS may have affected the chloride-induced currents indirectly by inhibiting the V-ATPase activity. Therefore experiments using another general inhibitor of chloride-conducting proteins NPPB were performed. In contrast to DIDS, NPPB inhibited the vesicular chloride currents but not the V-ATPase-related currents. Despite these observations, a direct inhibition of the chloride conductance with DIDS is possible. Such a direct inhibition is especially interesting in the light of the new finding that the DIDS-sensitive glutamate transporter VGLUT1 is essential for the acidification of synaptic vesicles [5, 16, 38]. This finding suggests that VGLUT1 represents the major chloride permeation pathway in synaptic vesicles. However, other chloride conducting proteins have also been demonstrated to play a role in the acidification of synaptic vesicles [22, 23, 39]. Therefore, the chloride-induced currents detected with the SSM-based approach may represent activities of different vesicular chloride-conducting proteins. Further combined studies using the SSM-based technology and acidification assays may help to elucidate the significance of these currents for the acidification of the vesicles *in vivo*.

*Conclusions.* During the last decade SSM-based electrophysiological studies on different transporters, pumps and channels have accumulated demonstrating the wide applicability of the technology for the transport protein research [11, 13, 40, 41]. Here, the described approach expands the applicability of the SSM-based electrophysiology to ATPases of synaptic vesicles and plasma membranes. The protocols allowed detailed mechanistic and pharmacological characterization of the vesicular V-ATPase as well as plasma membrane $Na^+/K^+$-ATPase, and enabled discriminating between the activities of these two proteins in their native surroundings. Together with protocols for measuring neurotransmitter transporters such as the glutamate transporter EAAC1 [42] future SSM studies can help to understand the complex interplay of these proteins in synaptic signalling.

**Acknowledgements**

We gratefully acknowledge Klaus Fendler and Karin Schumacher for their critical reading of the manuscript, and Wolf Berger for his excellent technical assistance. We thank Robin Krause for providing Fig. 1.

**References**


1 Blanco, G. and Mercer, R. W. (1998) Isozymes of the Na-K-ATPase: heterogeneity in structure, diversity in function. Am J Physiol. **275**, F633-650

2 Beyenbach, K. W. and Wieczorek, H. (2006) The V-type H+ ATPase: molecular structure and function, physiological roles and regulation. J Exp Biol. **209**, 577-589

3 Takamori, S., Holt, M., Stenius, K., Lemke, E. A., Gronborg, M., Riedel, D., Urlaub, H., Schenck, S., Brugger, B., Ringler, P., Muller, S. A., Rammner, B., Grater, F., Hub, J. S., De Groot, B. L., Mieskes, G., Moriyama, Y., Klingauf, J., Grubmuller, H., Heuser, J., Wieland, F. and Jahn, R. (2006) Molecular anatomy of a trafficking organelle. Cell. **127**, 831-846

4 Cidon, S. and Sihra, T. S. (1989) Characterization of a H+-ATPase in rat brain synaptic vesicles. Coupling to L-glutamate transport. J Biol Chem. **264**, 8281-8288

5 Schenck, S., Wojcik, S. M., Brose, N. and Takamori, S. (2009) A chloride conductance in VGLUT1 underlies maximal glutamate loading into synaptic vesicles. Nat Neurosci. **12**, 156-162

6 Davies, J. M., Hunt, I. and Sanders, D. (1994) Vacuolar H(+)-pumping ATPase variable transport coupling ratio controlled by pH. Proc Natl Acad Sci U S A. **91**, 8547-8551

7 Pintschovius, J. and Fendler, K. (1999) Charge translocation by the Na+/K+-ATPase investigated on solid supported membranes: rapid solution exchange with a new technique. Biophys J. **76**, 814-826

8 Ahdut-Hacohen, R., Duridanova, D., Meiri, H. and Rahamimoff, R. (2004) Hydrogen ions control synaptic vesicle ion channel activity in Torpedo electromotor neurones. J Physiol. **556**, 347-352

9 Rahamimoff, R., DeRiemer, S. A., Sakmann, B., Stadler, H. and Yakir, N. (1988) Ion channels in synaptic vesicles from Torpedo electric organ. Proc Natl Acad Sci U S A. **85**, 5310-5314

10 Friedrich, T., Bamberg, E. and Nagel, G. (1996) Na+,K(+)-ATPase pump currents in giant excised patches activated by an ATP concentration jump. Biophys J. **71**, 2486-2500

11 Schulz, P., Garcia-Celma, J. J. and Fendler, K. (2008) SSM-based electrophysiology. Methods

12 Weitz, D., Harder, D., Casagrande, F., Fotiadis, D., Obrdlik, P., Kelety, B. and Daniel, H. (2007) Functional and structural characterization of a prokaryotic peptide transporter with features similar to mammalian PEPT1. J Biol Chem. **282**, 2832-2839

13 Kelety, B., Diekert, K., Tobien, J., Watzke, N., Dorner, W., Obrdlik, P. and Fendler, K. (2006) Transporter assays using solid supported membranes: a novel screening platform for drug discovery. Assay Drug Dev Technol. **4**, 575-582

14 Morciano, M., Burre, J., Corvey, C., Karas, M., Zimmermann, H. and Volknandt, W. (2005) Immunoisolation of two synaptic vesicle pools from synaptosomes: a proteomics analysis. J Neurochem. **95**, 1732-1745

15 Morciano, M., Beckhaus, T., Karas, M., Zimmermann, H. and Volknandt, W. (2009) The proteome of the presynaptic active zone: from docked synaptic vesicles to adhesion molecules and maxi-channels. J Neurochem. **108**, 662-675

16 Hartinger, J. and Jahn, R. (1993) An anion binding site that regulates the glutamate transporter of synaptic vesicles. J Biol Chem. **268**, 23122-23127

17 Bowman, E. J., Siebers, A. and Altendorf, K. (1988) Bafilomycins: a class of inhibitors of membrane ATPases from microorganisms, animal cells, and plant cells. Proc Natl Acad Sci U S A. **85**, 7972-7976

18 Berrebi-Bertrand, I., Maixent, J. M., Guede, F. G., Gerbi, A., Charlemagne, D. and Lelievre, L. G. (1991) Two functional Na+/K(+)-ATPase isoforms in the left ventricle of guinea pig heart. Eur J Biochem. **196**, 129-133

19 Drose, S. and Altendorf, K. (1997) Bafilomycins and concanamycins as inhibitors of V-ATPases and P-ATPases. J Exp Biol. **200**, 1-8

20 Kettner, C., Obermeyer, G. and Bertl, A. (2003) Inhibition of the yeast V-type ATPase by cytosolic ADP. FEBS Lett. **535**, 119-124

21 Yabe, I., Horiuchi, K., Nakahara, K., Hiyama, T., Yamanaka, T., Wang, P. C., Toda, K., Hirata, A., Ohsumi, Y., Hirata, R., Anraku, Y. and Kusaka, I. (1999) Patch clamp studies on V-type ATPase of vacuolar membrane of haploid Saccharomyces cerevisiae. Preparation and utilization of a giant cell containing a giant vacuole. J Biol Chem. **274**, 34903-34910

22 Jentsch, T. J., Stein, V., Weinreich, F. and Zdebik, A. A. (2002) Molecular structure and physiological function of chloride channels. Physiol Rev. **82**, 503-568

23 Stobrawa, S. M., Breiderhoff, T., Takamori, S., Engel, D., Schweizer, M., Zdebik, A. A., Bosl, M. R., Ruether, K., Jahn, H., Draguhn, A., Jahn, R. and Jentsch, T. J. (2001) Disruption of ClC-3, a chloride channel expressed on synaptic vesicles, leads to a loss of the hippocampus. Neuron. **29**, 185-196

24 David, P. and Baron, R. (1994) The catalytic cycle of the vacuolar H(+)-ATPase. Comparison of proton transport in kidney- and osteoclast-derived vesicles. J Biol Chem. **269**, 30158-30163

25 Johnson, R. G., Beers, M. F. and Scarpa, A. (1982) H+ ATPase of chromaffin granules. Kinetics, regulation, and stoichiometry. J Biol Chem. **257**, 10701-10707

26 Gropp, T., Cornelius, F. and Fendler, K. (1998) K+-dependence of electrogenic transport by the NaK-ATPase. Biochim Biophys Acta. **1368**, 184-200

27 Scheiner-Bobis, G., Esmann, M. and Schoner, W. (1989) Shift to the Na+ form of Na+/K+-transporting ATPase due to modification of the low-affinity ATP-binding site by Co(NH3)4ATP. Eur J Biochem. **183**, 173-178

28 Pintschovius, J., Fendler, K. and Bamberg, E. (1999) Charge translocation by the Na+/K+-ATPase investigated on solid supported membranes: cytoplasmic cation binding and release. Biophys J. **76**, 827-836

29 Post, R. L., Hegyvary, C. and Kume, S. (1972) Activation by adenosine triphosphate in the phosphorylation kinetics of sodium and potassium ion transport adenosine triphosphatase. J Biol Chem. **247**, 6530-6540

30 Saurin, A. J., Hamlett, J., Clague, M. J. and Pennington, S. R. (1996) Inhibition of mitogen-induced DNA synthesis by bafilomycin A1 in Swiss 3T3 fibroblasts. Biochem J. **313 ( Pt 1)**, 65-70

31 Yoshimori, T., Yamamoto, A., Moriyama, Y., Futai, M. and Tashiro, Y. (1991) Bafilomycin A1, a specific inhibitor of vacuolar-type H(+)-ATPase, inhibits acidification and protein degradation in lysosomes of cultured cells. J Biol Chem. **266**, 17707-17712

32 Xie, X. S., Padron, D., Liao, X., Wang, J., Roth, M. G. and De Brabander, J. K. (2004) Salicylihalamide A inhibits the V0 sector of the V-ATPase through a mechanism distinct from bafilomycin A1. J Biol Chem. **279**, 19755-19763

33 Zhang, J., Feng, Y. and Forgac, M. (1994) Proton conduction and bafilomycin binding by the V0 domain of the coated vesicle V-ATPase. J Biol Chem. **269**, 23518-23523

34 Guizouarn, H., Gabillat, N., Motais, R. and Borgese, F. (2001) Multiple transport functions of a red blood cell anion exchanger, tAE1: its role in cell volume regulation. J Physiol. **535**, 497-506

35 Wilson, M. C., Meredith, D., Bunnun, C., Sessions, R. B. and Halestrap, A. P. (2009) Studies on the dids binding site of monocarboxylate transporter 1 suggest a homology model of the open conformation and a plausible translocation cycle. J Biol Chem

36 Armbruster, A., Hohn, C., Hermesdorf, A., Schumacher, K., Borsch, M. and Gruber, G. (2005) Evidence for major structural changes in subunit C of the vacuolar ATPase due to nucleotide binding. FEBS Lett. **579**, 1961-1967

37 Webster, L. C. and Apps, D. K. (1996) Analysis of nucleotide binding by a vacuolar proton-translocating adenosine triphosphatase. Eur J Biochem. **240**, 156-164

38 Bellocchio, E. E., Reimer, R. J., Fremeau, R. T., Jr. and Edwards, R. H. (2000) Uptake of glutamate into synaptic vesicles by an inorganic phosphate transporter. Science. **289**, 957-960

39 Li, X., Shimada, K., Showalter, L. A. and Weinman, S. A. (2000) Biophysical properties of ClC-3 differentiate it from swelling-activated chloride channels in Chinese hamster ovary-K1 cells. J Biol Chem. **275**, 35994-35998

40 Ganea, C. and Fendler, K. (2009) Bacterial transporters: Charge translocation and mechanism. Biochim Biophys Acta

41 Garcia-Celma, J. J., Smirnova, I. N., Kaback, H. R. and Fendler, K. (2009) Electrophysiological characterization of LacY. Proc Natl Acad Sci U S A. **106**, 7373-7378

42 Krause, R., Watzke, N., Kelety, B., Dorner, W. and Fendler, K. (2009) An automatic electrophysiological assay for the neuronal glutamate transporter mEAAC1. J Neurosci Methods. **177**, 131-141

**Figure legends**

**Fig. 1:** Arrangement of vesicles (left) and membrane fragments (right) on the sensors and the corresponding equivalent electrical circuits. "TR" is the transport protein embedded in the vesicle membrane (M) or in the membrane fragment (M). The arrows indicate the translocation of positive charges into the fluid compartments between the biological membranes M and the SSM. The charging of the compartments results in charging of the gold electrode (E). The SSM consists of an upper phospholipid layer and a lower alkane thiol layer residing on E.

**Fig. 2:** ATP-induced acidification of synaptic vesicles measured as the quenching of acridine orange (AO) fluorescence. The acidification was induced by 120 µM ATP (arrow). **A**: Acidification of synaptic vesicles (SV, ▼) was prevented by pre-incubating the vesicles with 25 nM bafilomycin A1 (BafA1, ∇). No acidification was detected with synaptic plasma membranes (SPM, ■ and □). SV correspond to sucrose gradient fractions F5 to F9, SPM to fractions F24 to F26. **B**: Inhibition of SV acidification with DIDS and CCCP. For the two upper traces, 10 µM DIDS (○) or 20 µM CCCP (▲) were applied prior to the addition of 120 µM ATP. In the lower trace (Δ), the acidification was reverted by the application of 20 µM CCCP 10 min after ATP application. Each trace is representative of ≥4 independent experiments.

**Fig. 3:** V-ATPase-specific currents induced by ATP-concentration jumps on sensors covered with SV (fractions F5-F9). The currents were induced by fast exchange of an ATP-free solution for a solution containing 0-1000 µM ATP. The upper bar indicates the solution exchange. If not stated, the solutions contained 2 mM $Mg^{2+}$. All experiments were performed in $Na^+$-free conditions. **A**: ATP (300 µM) induced magnesium-dependent electrical currents. For $Mg^{2+}$-free conditions 0.5 mM EDTA was added to the solutions. **B**: Inhibition of the ATP-induced currents with the V-ATPase-inhibitor BafA1. **C** and **D**: Dependence of the signal amplitudes on the applied ATP concentration. The amplitudes (peak currents) were normalized relative to the peak currents at 1000 µM ATP. The $K_{0.5}$ was calculated by fitting the current amplitudes at different ATP concentrations using Michaelis-Menten kinetics. Concentrations are shown at logarithmic scale. N = 3-5 (± SEM) for data points at each concentration.

**Fig. 4** $Na^+/K^+$-ATPase-specific currents on sensors covered with SPM (**A** and **B**) and the distribution of V-ATPase and $Na^+/K^+$-ATPase activities in sucrose gradient fractions (**C**). **A**: Currents were induced by rapid solution exchange using 150 µM ATP on SPM sensors under $Na^+$-containing but $K^+$-free conditions. The currents were inhibited by digitoxigenin (Dig) but not by BafA1. The upper bar indicates the solution exchange. **B**: ATP dependence of the Dig-sensitive currents in SPM at $K^+$-free conditions. The $K_{0.5}$ was determined by fitting a sigmoidal dose response kinetic to the data (n = 6 ± SEM for each concentration). **C**: Distribution of BafA1-(white) and Dig-sensitive (striped) ATP signals (150 µM) in sucrose gradient fractions F6 to F8 (SV), F14 (intermediate fraction) and F24 and F26 (SPM). Black bars correspond to ATP-induced signals without inhibitors. The white and stripped bars correspond to the residual currents after the application of the respective inhibitor. No significant ATP-induced currents were detected in F14. BafA1 was 10 nM, Dig 1 µM. Bars are mean (±SEM) of 3-5 independent experiments.

**Fig. 5**: Kinetics of V-ATPase inhibition with BafA1, DIDS and ADP. Sensors were prepared with SV (fractions F5-F8). The graphs show peak currents normalized to the peak currents recorded at 100 µM ATP (**A** and **B**) or 120 µM ATP (**C** and **D**) in absence of BafA1, DIDS or ADP. **A**: Time- and dose-dependence of the BafA1 inhibition. The currents were repeatedly induced by 100 µM ATP. After 30 min, 1 nM (■) or 5 nM (○) BafA1 were applied and the currents were recorded for another 40-50 min. Finally, inhibitor-free solutions were used again (washout). Each data point represents the mean of two independent experiments. The inset shows sequential application of increasing BafA1 concentrations on one SV-loaded sensor. **B**: Inhibition of V-ATPase with DIDS. The currents were repeatedly induced by 100 µM ATP concentration jumps. After 20 min, 0.1 (○), 1 (▲), or 10 (■) µM DIDS was supplied to the solutions, and the V-ATPase activity was recorded for another 15 to 50 min. **C**: Inhibition of V-ATPase with ADP. V-ATPase was activated by 120 µM ATP. The $IC_{50}$ for ADP was determined by fitting a sigmoidal dose response kinetic to the data (n = 5 ± SEM for each concentration). **D**: Washout of ADP. The graph shows V-ATPase-specific currents at 120 µM ATP before ADP application (left black bar), in presence of 1, 10 or 100 µM ADP (striped, dotted and white bars), and after the washout of the corresponding ADP

concentration (intermediate black bars). Each bar is a mean (± SEM) of 3-5 independent experiments.

**Fig. 6**: Simultaneous measurements of the V-ATPase-specific and chloride-induced currents from SV (fractions F5-F8) and inhibition by DIDS and NPPB. The upper bars indicate the flow of the ATP- and the chloride-containing solutions. **A**: Stimulation of chloride-induced currents by V-ATPase. Upper trace: Chloride conductance was induced in absence of ATP by exchanging chloride-free solutions for the solution containing 30 mM $Cl^-$. Lower trace: V-ATPase was activated by exchanging the ATP- and chloride-free pre-incubating solution for the solution containing 300 µM ATP. Subsequently, the chloride conductance was induced by applying 30 mM KCl as described for upper trace. **B** and **C**: Effects of DIDS (1, 10, 100 µM) and NPPB (10 µM) on V-ATPase and on chloride conductance. The experiments were performed as described in A. Different concentrations of DIDS or NPPB were used. For **A**, **B** and **C**: Each trace is representative of ≥4 independent experiments. **D:** Quantitative analysis of DIDS (1, 10, 100 µM) and NPPB (10 µM, white bar) effects on chloride conductance. The chloride-induced signals in presence of inhibitors were normalized relative to the signals in absence of inhibitors (black bar). Each bar is a mean (± SEM) of ≥4 independent experiments.

Figure 1

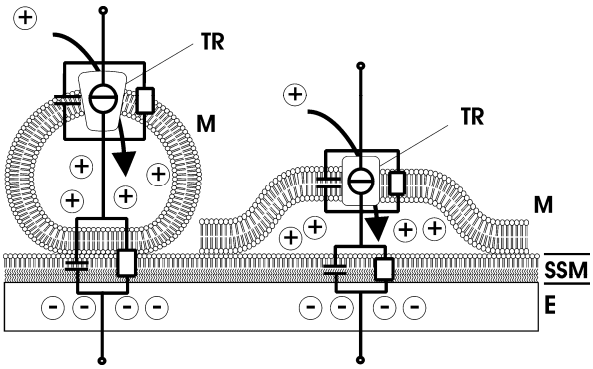

Figure 2

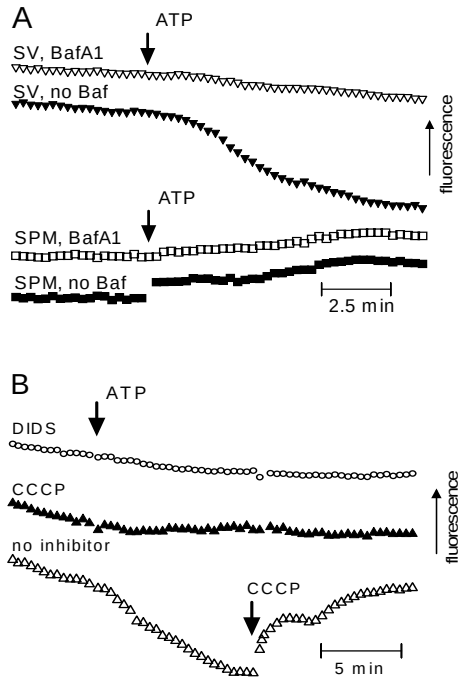

Figure 3

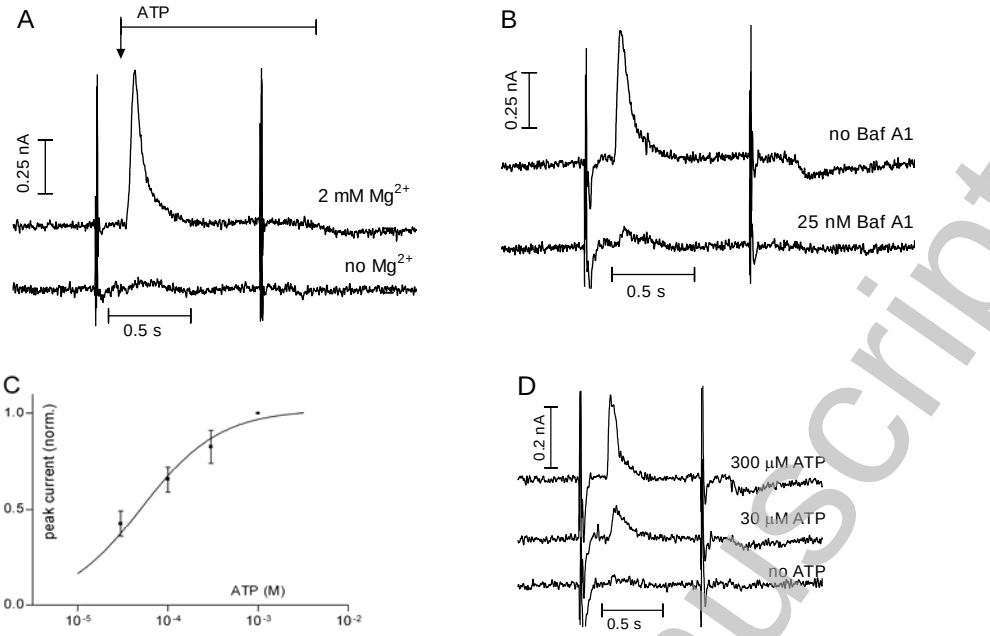

Figure 4

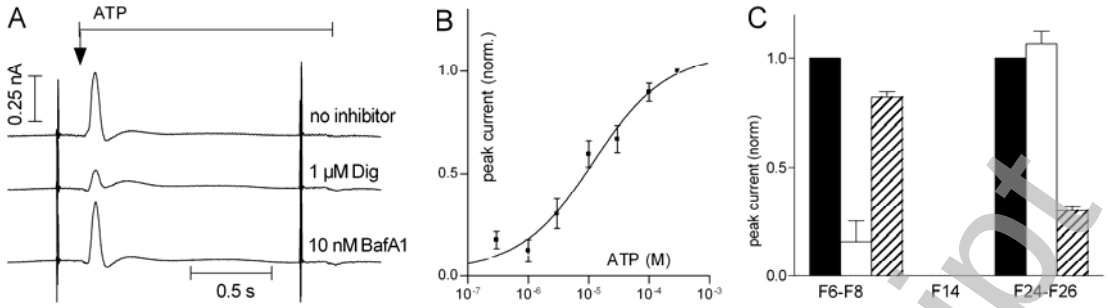

Biochemical Journal Immediate Publication. Published on 25 Jan 2010 as manuscript BJ20091380

Figure 5

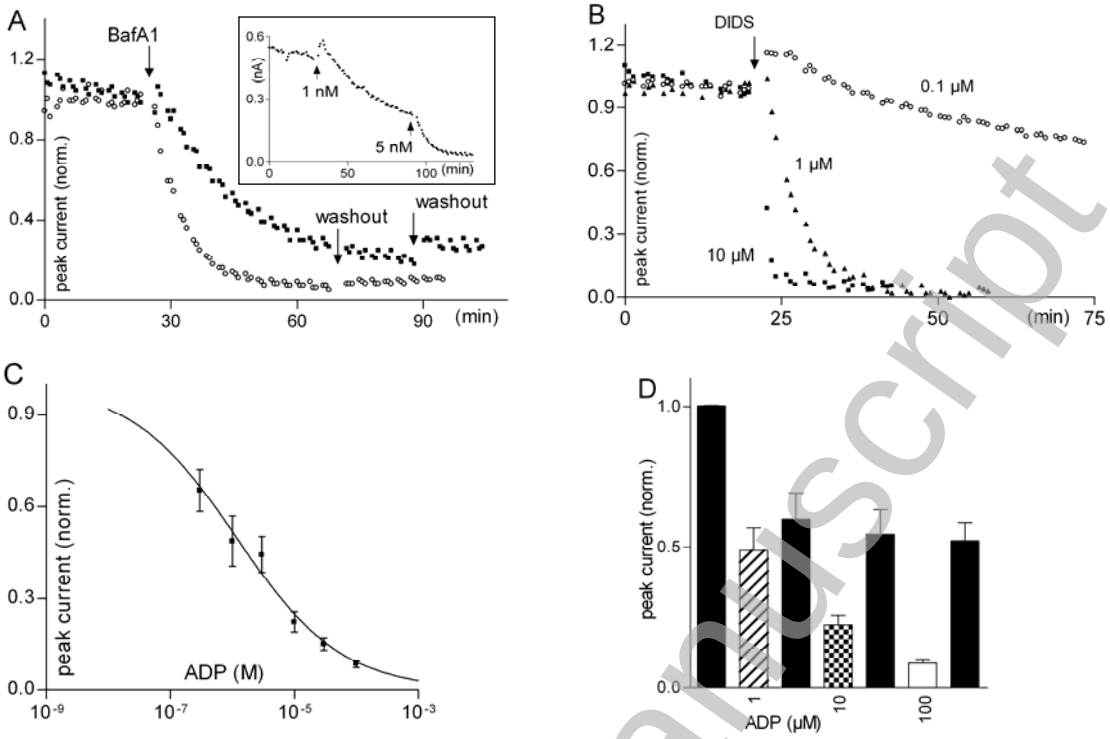

Figure 6